

**N000141712334 : Air-Sea Coupling in Monsoon Intraseasonal Oscillations****Reporting Period:** JUN 16, 2020 to JUN 15, 2021**Date Received:****Submitter:** Harindra Fernando

---

**Distribution Statement:** Approved for public release; distribution is unlimited.

---

**Major Goals**

Reliable predictions of the initiation, propagation, strength, and variability of Monsoon Intraseasonal Oscillations (MISO) constitute building blocks of monsoon forecasts, which are crucial for ensuring the socioeconomic wellbeing and safety of nearly one billion inhabitants of the Indian subcontinent. MISO are sub-seasonal weather phenomena that originate in the tropics, propagate predominantly northward over the Bay of Bengal (BOB) and then move both northward and westward over the southeast Asian landmass. Active and break phases of monsoons are directly correlated with MISO, but significant biases and errors in current forecasts have been a bane for socioeconomic planning and risk assessment beyond several weeks in advance. Mounting evidence suggests that accurate accounting of air-sea coupling is imperative for skillful forecasting of MISO and attendant outcomes such as rainfall, yet our lack of understanding of thermodynamic and physical processes, both on the ocean and atmospheric sides, has stymied the progress of forecast improvements. MISOs are a meld of multiscale physical processes working symbiotically to produce organized, migrating rain bands separated by periods of clear sky.

This project seeks to study critical science questions underlying MISO dynamics. Of particular interest are the physical mechanisms responsible for heat, momentum and mass transfer across the air-sea interface, feedbacks between atmospheric and oceanic boundary layers, lead-lag relationships the sea-surface temperature (SST), net heat flux and precipitation, as well as sustaining and decaying of MISO convection. Collectively, a suite of high-end atmospheric and oceanic instrumentation was deployed in the Indian Ocean, on the land over multiple countries, aboard research vessels and on an aircraft to collect data of high granularity. Ultra-high resolution coupled numerical simulations are being used to guide field experimental designs and data interpretation. Novel autonomous measurement platforms and large eddy simulation (LES) technologies were to be developed to study MISO-relevant air-sea processes. Satellite and reanalysis products are used to augment in situ data, allowing integration of observations across sub-meso to seasonal scales. In unison, the project will contribute to improved forecasts of MISO, and Monsoons in general, via discovery of physical mechanisms, understanding their linkages, development of model-relevant parameterizations, and providing a robust dataset for modelers. Collaboration with government agencies from the US and partnering countries (Sri Lanka, Maldives, Singapore and Seychelles) will help transition research to forecasting products. The project includes capacity building of partnering countries, Sri Lanka, Seychelles and Maldives.

As mentioned in the previous reports, the past major activities (2017-2020) included: (i) Participation in the Leg-2 of the 2018 MISO-BOB field campaign based on R/V Tommy G. Thompson. The cruises included two legs, Leg 1 during 4-23 June out of Chennai and Leg 2 during 30 June-29 July out of Colombo, Sri Lanka. (ii) Orchestrating and conducting a C-130 aircraft campaign conducted by the U.S. Air Force Weather Research Squadron WRS 53 (Hurricane Hunters). The campaign included four legs: Flight 1 – 15 June; Flight 2 – 17 June; Flight 3 – 18 June; and Flight 4 – 01 July, 2018. The flights operated out of Bandaranayke International Airport,

Colombo, Sri Lanka. These flights performed a dropsonde surveys along equatorial and north-south transects, and deployed profiling floats and surface drifters. (iii) Participated in the 2019 field campaign (27 May to 04 July, 2019) based on R/V Sally Ride. This included two cruise legs: Leg 1 out of Phuket, Thailand during 27 May to 26 June (focused on recovery of a moored array for Naval Research Laboratory (NRL). The cruises performed air-sea and remote sensing measurements in support of MISO studies and sampled Sri Lankan coastal waters. Leg 2 was out of Chennai, India during 06 July to 05 August. (iv) Deployment of remote sensor and flux tower suites in Sri Lanka, Maldives and Seychelles during the 2019 field campaigns. Indian Meteorological Department (IMD) conducted additional high frequency sounding at a number of land locations. (v) Analysis of data from both field campaigns. (vi) Conduct of high-resolution, turbulence-resolving large-eddy simulation (LES) to elucidate the dynamics of air-sea interaction at the scales of marine atmospheric boundary layer (MABL). Computational resources provided by the DoD High-Performance Computing Centers and NCAR were utilized to carry out cutting edge simulations using ~1010 meshes (NCAR contribution).

Continuing this research, the 2020-2021 tasks included: (i) Complete the analysis of an anomalous meteorological event in Sri Lanka occurred on 18 July 2019, invoking the effects of intraseasonal planetary waves, and preparation of a journal manuscript. (ii) Complete the analysis of propagating weather disturbances across Bay of Bengal triggered by convectively coupled equatorial waves during the 2019 southwest monsoon and preparation of a journal manuscript. (iii) Study the response of MABL to heterogeneous sea surface temperature (SST) gradients and document results in two published papers (NCAR contribution). (iv) Participate in several journal manuscript preparations and submittals, including a BAMS paper on monsoon onset during MISO-BOB. Some of these are already accepted. (v) Participate in the MISO-BOB webinar series and review meetings.

---

## Accomplishments Under Goals

(1) Analysis of an anomalous weather event: During 2019 MISO-BOB summer field campaign (27 May to 31 July), a comprehensive array of ground stations was deployed in Sri Lanka, Maldives, and Seychelles, including Doppler Lidars, flux towers, ceilometers and radiosoundings. At the WMO sites in Maldives and Sri Lanka, the sounding frequency was increased. The campaign included two MISO-BOB ocean cruises aboard R/V Sally Ride, from which soundings were made at 3/6-hour intervals. While MISOs were rare during the campaign period, intense weather anomalies of significant interest were observed with implications for air-sea interaction and weather forecasting studies. As mentioned, a noteworthy event occurred on July 18 in Sri Lanka, where unusual rainfall (>200 mm) was reported in the Southern and Central highland areas accompanied by winds of 70-80 km/hr lasting for several hours (Fig. 1). At first, Sri Lanka Meteorological Department attributed this to a passing baroclinic Kelvin wave, possibly its breakdown at a high altitude and transferring momentum downward. Analysis of high-resolution radiosonde data from Maldives and Sri Lanka (Fig. 1) alongside information from ERA-5 (Fig. 2) and TRMM satellite (Fig. 3) did not support this hypothesis. Instead ERA-5 and TRMM spectral signatures raised the possibility of an Equatorial Rossby (ER) wave propagating westward at a low altitude accompanied by the presence of convectively coupled Kelvin and ER waves. Strong Kelvin-wave signatures in the equatorial belt, however, were not related to the anomalous event in Sri Lanka, given the event-related disturbances were westward (Figs. 1 and 2). The ER wave appeared to be responsible for the event. (2) The role of SST gradients and large-scale meteorological forcing in propelling MISOs northward: MISOs originate in the equatorial belt south of BOB, and it is hypothesized that eastward equatorial planetary waves together with N-S SST gradients trigger northward propagation of MISO. To delve into this hypothesis, TRIMM satellite data (Fig. 4) and high frequency land-based radiosoundings conducted as part of MISO-BOB (Fig. 5) were analyzed. Fig. 4a indeed shows eastward equatorial disturbances with a speed 6.5 m/s (typical of convectively coupled equatorial waves) toward

maritime continent, their arrival at southern BoB with intraseasonal periodicity, followed by an initiation of a northward disturbance with 1-2 m/s, a characteristic of MISO (Fig. 4b). The vertical profiles of specific humidity in Fig. 5 add insights on moist convection within local weather. Port Blair located in BOB at (92E, 11N) in Fig. 5c is an example (assuming negligible orographic precipitation), where intraseasonal oscillations of moisture with an oscillation period of  $\sim 17$  days are evident (14 July to 30 July). Figure 5a shows the vertical atmospheric profiles for Trivandrum, the capital of Kerala, a critical location used by IMD to mark the onset (active) period of southwest monsoon. Intraseasonal oscillations of moisture are observed at both Trivandrum and Port Blair, but data drop out prevents making inferences from Chennai and Kolkata soundings. (3) Mixing parameters in BOB versus some other regions of the world: Oceanographic measurements carried out in June 2019 onboard R/V Sally Ride using VMP-500 microstructure profiler were analyzed (Fig. 6). The study focused on comprehensive statistical analyses of eddy diffusivities in the upper pycnocline and their comparisons with those obtained elsewhere: 2013 in the northern BoB (Jinadasa et al., *Oceanography* 29(2), 2016), 2014 along two sections to the south and west from Sri Lanka coast (Lozovatsky et al., *J. Geophys. Res. Oceans*, 122, 2017), 2018 in the western BoB in the area of Sri Lanka Dome (Lozovatsky et al., *Deep-Sea Res. Pt. II* 168, 2019), and in two deep-ocean regions of Gulf Stream GS in 2015 (Lozovatsky et al., *Ocean Dynamics*, 67(6), 2017) and Southern California Bight SCB in 2017 (Lozovatsky et al., *J. Geophys. Res., Oceans*, 124 2019). The influence of internal-wave instability on turbulence generation in the pycnocline of southern BOB was explored in the context of observed layered structure therein. All cumulative probability distribution functions CDF of diffusivity in the pycnocline could be well-fitted by generalized extreme value distribution GEVD, suggesting highly space-time intermittency of pycnocline mixing in general (Fig. 7). Statistics of mixing such as the median of diffusivity gradually decreased from the most southeastern BOB station (8N) toward that at 14N, and then sharply dropped at 16N affected by low-saline water inflow in the northern part of BOB. In all western stations of BOB located along 8N, the median diffusivity returns to its characteristic value  $2 \times 10^{-6} \text{ m}^2/\text{s}$  found in the central and eastern BOB. Some elevated values were associated with the Sri Lanka Dome, indicating possible mixing enhancement associated with mesoscale ocean dynamics. Diffusivity statistics in the upper pycnocline of SCB and GS are similar to those of southern BOB, showing relatively low diffusivities compared to the canonical diffusivity  $10^{-6} \text{ m}^2/\text{s}$  suggested decades ago based on measurements in central Atlantic (Tool et al., *Science*, 264, 1994). (4) LES of weakly convective MABL subjected to heterogeneous SST gradients and geostrophic winds: A single-sided warm or cold front with temperature jumps = (2, -1.5)K varying over a horizontal distance of 1 km, characteristic of an upper ocean mesoscale or submesoscale front, was used with geostrophic wind (10 m/s) oriented either perpendicular (across front) or parallel (down front) to the SST. With down-front winds the ageostrophic surface wind was weak, about 5 times smaller than the geostrophic wind with horizontal pressure gradients coupling SST front and the atmosphere in the momentum budget. With across front winds, horizontal pressure gradients are weak and mean horizontal advection primarily balanced the vertical flux divergence. Down front winds generate persistent secondary circulations SC that modify the surface and interior MABL turbulent fluxes depending on the sign of the temperature front; Fig. 8. Warm filaments are generated by a pair of cold-warm and warm-cold fronts separated by a small finite distance; swapping the horizontal position of the fronts generated a cold filament. Filaments developed opposing pairs of SC with a central upwelling or downwelling region between the cells. Cold filaments reduced the entrainment near the boundary-layer top, which may impact cloud initiation. The exploration of the effects of currents on the MABL was initiated. A typical circular water eddy with azimuthal speed  $\sim 1$  m/s and varying radius between 400 and 2000 m is imposed as a lower boundary condition in LES. The eddy has solid body cyclonic rotation that decays exponentially in the far field. Important impacts of the MABL-current coupling depending on the wind speed and eddy radius were noted. In the case of free convection (no mean wind) a very coherent thermal plume is generated at the center of the LES domain that reaches to the top of the MABL. The azimuthal winds in the plume are cyclonic with

strong inward radial winds converging at the plume center, driving vertical motions. The results are sensitive to the thermal boundary condition (e.g., fixed SST or surface flux). Fixed SST boundary generates the most coherent plume. A weakly convective MABL with geostrophic winds also responds to surface currents. A dipole in the surface wind stress is observed above the water eddy; the magnitude of the wind stress increases as the radius of the eddy increases, at the same time as the winds decrease. A similar dipole is found in the surface temperature flux because of coupling with the wind stress (Fig. 9). Tails of the probability density functions (PDFs) of the surface temperature flux widen in the presence of the water eddy.

---

### **Plans Next Period**

During the next reporting period, it is planned to: (i) hire a post-doc to analyze C-130 aircraft data taken during the MISO-BOB 2018 campaign, delving into the structure of convective events, convergence and divergence regions and SST gradients; (ii) continue analysis of data from 2018/2019 MISO-BOB cruises, ground stations and from high-frequency radiosoundings from the IMD; (iii) Submit a paper dealing with July 18, 2019 anomalous weather event in Sri Lanka and another on MISO Propagation deduced from land/ship soundings and TRMM results; (iv) ramp up LES on the effects of ocean currents on the MABL, (v) Continue collaboration with NRL-Stennis and NRL-Monterey; (vi) enhance collaboration with other MISO-BOB participants via small-group meetings and by participation in MISO-BOB webinar series, (vi) publication of related results in archival journals; (vii) presentation of results at national/international meetings and project overview workshops; (viii) re-start the exchange program with scientists from Sri Lanka, Seychelles and Maldives after a hiatus period during Covid-19.

---

### **Results Dissemination**

Major platforms for dissemination of results are national and international meetings, seminars, and peer-reviewed publications. The project involves many universities and national laboratories, and effective communication and reaching out to them are an important part of the project. Owing to Covid-19 protocols, out-of-state travel was completely restricted for researchers of all participating institutions, and zoom calls were used as the tool for project coordination and collaborative activities. Five (on-line) invited seminars on the project were made, at University of Wisconsin (Weston Lecture, Nelson Environmental Institute), Duke University, California Institute of Technology (Guggenheim Aeronautical Laboratory), Ocean University of Sri Lanka, and at Ramaiah University of Applied Sciences (Distinguished Lecture), Bangalore, India.

---

### **Honors and Awards**

Nothing to Report

---

### **Training Opportunities**

The training aspect of the work included supervision of two PhD students at Notre Dame (Edgar Gonzales and Jaynise Perez), a PhD candidate from the Ruhuna University, Sri Lanka (Mr. Priyantha Jinadasa), an M.Phil. Candidate from the National Aquatic Resources Research and Development Agency NARA, Sri Lanka (Udeshika Wimalasiri), a post-doctoral fellow at Notre Dame (Sandeep Wagh), a research engineer (Scott Coppersmith) and field technician (Orson Hyde)

at Notre Dame. Udeshika Wimalasiri completed the M.Phil degree, Jaynise Perez passed the PhD comprehensive exam in April 2021, and Priyantha Jinadasa submitted the PhD thesis to Ruhuna University in February 2021. Dr. Hemantha Wijesekera of NRL is in the supervisory committee for all graduate students, and the students have research collaboration with other DOD-laboratory personnel. Research Professor Iossif Lozovatsky, a participant of the MISO-BOB Project at Notre Dame, was also involved in student supervision. Jaynise Perez received a NOAA summer internship in 2021, working at the Silver Spring Campus. She also attended the NASA Summer School of ‘Using Satellite Observations to Advance Climate Models’ at JPL in Aug 2019 and was awarded an Internship by INDO-U.S. SCIENCE & TECHNOLOGY FORUM to conduct research at the Centre for Atmospheric and Oceanic Sciences (IISc) under the supervision of Professor G.N. Bhat (Sept 2019 – Nov 2019); this research collaboration continues to thrive. The students and junior researchers are provided with opportunities to present papers in national and international conferences. In all, early career researchers and graduate students received experience in deploying instruments from research vessels and on land, data processing, collaborative activities, conference presentations and preparation of research papers. Scott Coppersmith and Edward Creegan provided overall supervision for the Notre Dame group during the 2018 and 2019 MISO-BOB cruises whereas the PI supervised shore-based field work as well as academic work of the students. Junior researchers worked hand-in hand with senior personnel. Although the PI’s laboratory provides hands-on training for undergraduate students, due to Covid-19 restrictions no undergraduate research training was possible during 2020-21.

---

## Technology Transfer

The Lidar stabilizing platform developed for ONR CASPER-West and MISO-BOB (2018 Pilot) projects was discussed in previous reports, and over the past year its design was improved and significant changes were made to hardware and software with the hope of future deployments. Throughout the entire project, the PI maintained close collaboration with DOD laboratories, including Naval Research Laboratory (Stennis and Monterey), Army Research Laboratory (White Sands Missile Range, New Mexico) and 53d Weather Reconnaissance Squadron (403d Wing) of the US Air Force (Hurricane Hunters). During 10 to 30 June 2018, a WC-130J aircraft was deployed by the Hurricane Hunters as a part of the MISO-BOB project, with the PI handling agreements between the US and Sri Lanka. The collaboration with DOD laboratories is well evident from the publications reported herein.

---

## Participants

<b>Name</b>	<b>Role</b>	<b>Person Months</b>
Sullivan, Peter	Co PD/PI	3
Lozovatsky, Iossif	Faculty	3
Gonzales, Edgar	Graduate Student (research assistant)	12
Jinadasa, Udaya	Graduate Student (research assistant)	3
Perez, Jaynise	Graduate Student (research assistant)	12
Wimalasiri, Udeshika	Graduate Student (research assistant)	6
Coppersmith, Ronald	Other Professional	1
Creegan, Edward	Other Professional	1

Fernando, Harindra	PD/PI	2
Wagh, Sandeep	Postdoctoral (scholar, fellow or other postdoctoral position)	4
Hyde, Jay	Technician	1

**Figures: (Accomplishments/Progress)**

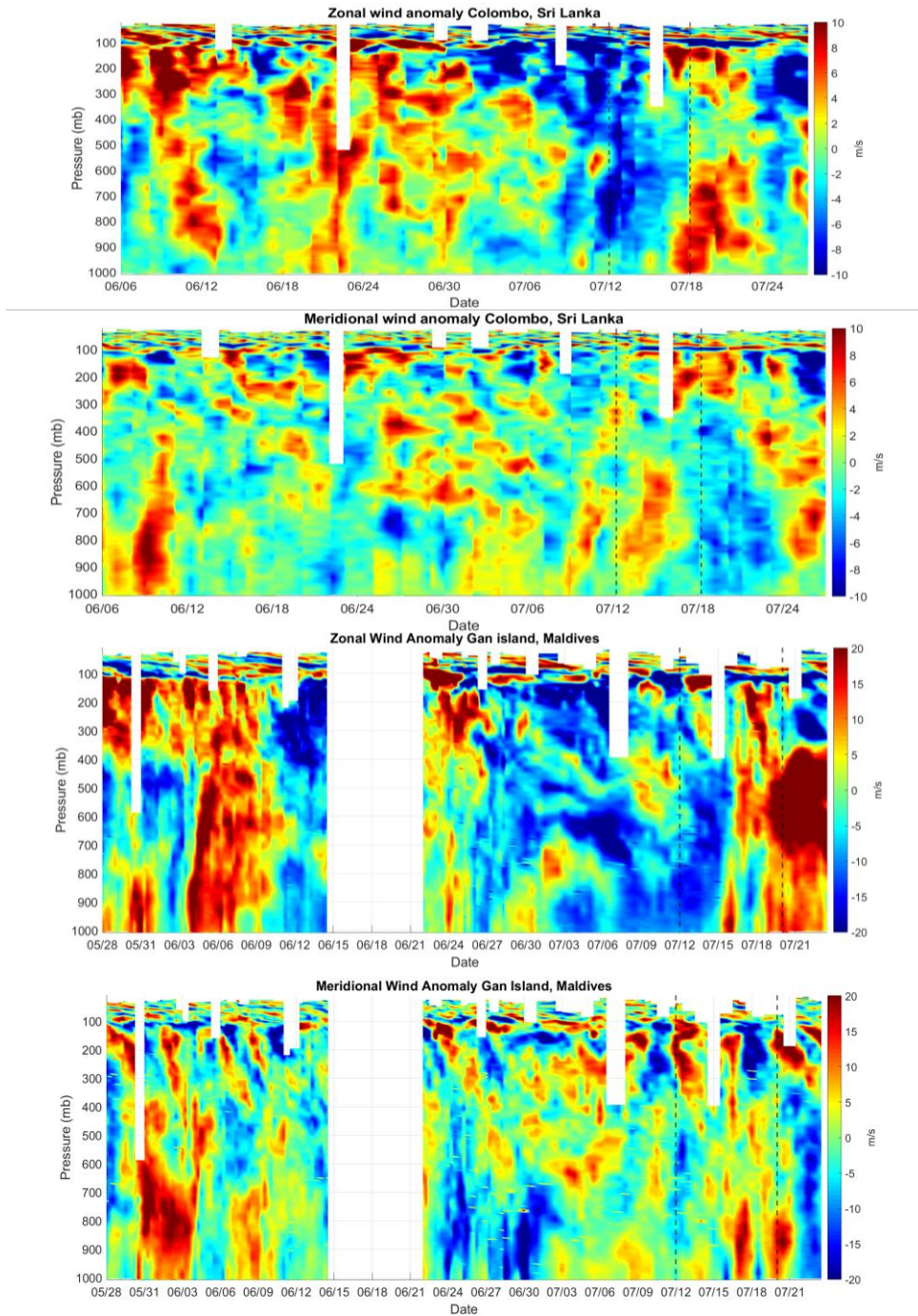


Figure 1: Time series of Zonal and Meridional wind anomalies from Radiosonde sounding in Sri Lanka and Maldives from late May to July 2019. Figure includes vertical profiles of zonal and meridional wind anomalies for Colombo, Sri Lanka and Gan Island, Maldives. Vertical dashed lines on Colombo plots show the dates of 12 and 18 July in which notable anomalies were observed. Vertical dashed lines on Gan Island plots mark 12 and 19 July in which notable anomalies were observed. This particular anomalous event is observed to be propagating westward (From Colombo toward Gan Island)

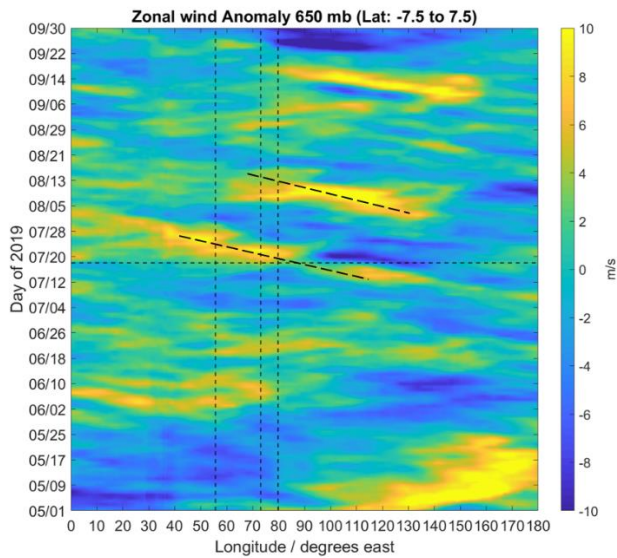


Figure 2: Hovmöller diagrams for zonal wind anomaly calculated from ERA-5 data products at pressure level 650 mb for the months of May-September, 2019 for longitudes 0E-180E.

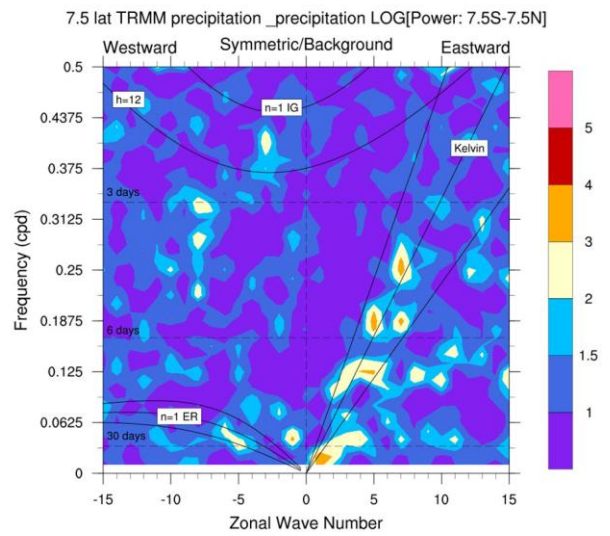


Fig. 3: Space time spectra symmetric component divided by background power spectra for TRMM dataset. Data spans the entire longitudinal band and 7.5°S-7.5°N domain.

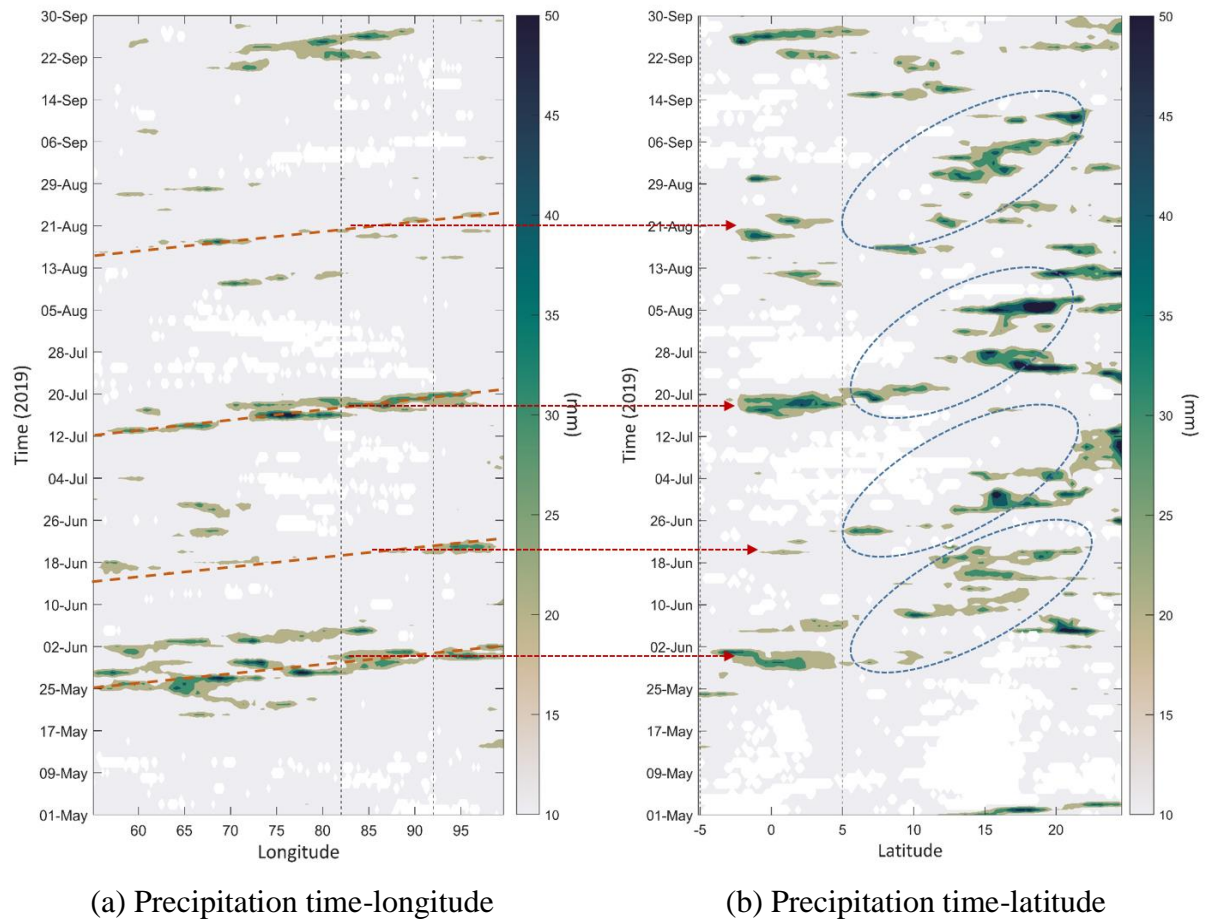


Figure 4: Time evolution of TRMM accumulated rainfall as a function of longitude(a) and latitude (b), respectively. Dashed vertical lines indicate the BOB domain (-5-5N, 82-92E). Bands of precipitation propagation are marked by dashed orange lines in (a) with red arrows indicating their respective locations in southern BOB. Blue ovals in (b) indicate the perceived northward propagation of precipitating bands through BOB from the initial band indicated by the red arrowhead.

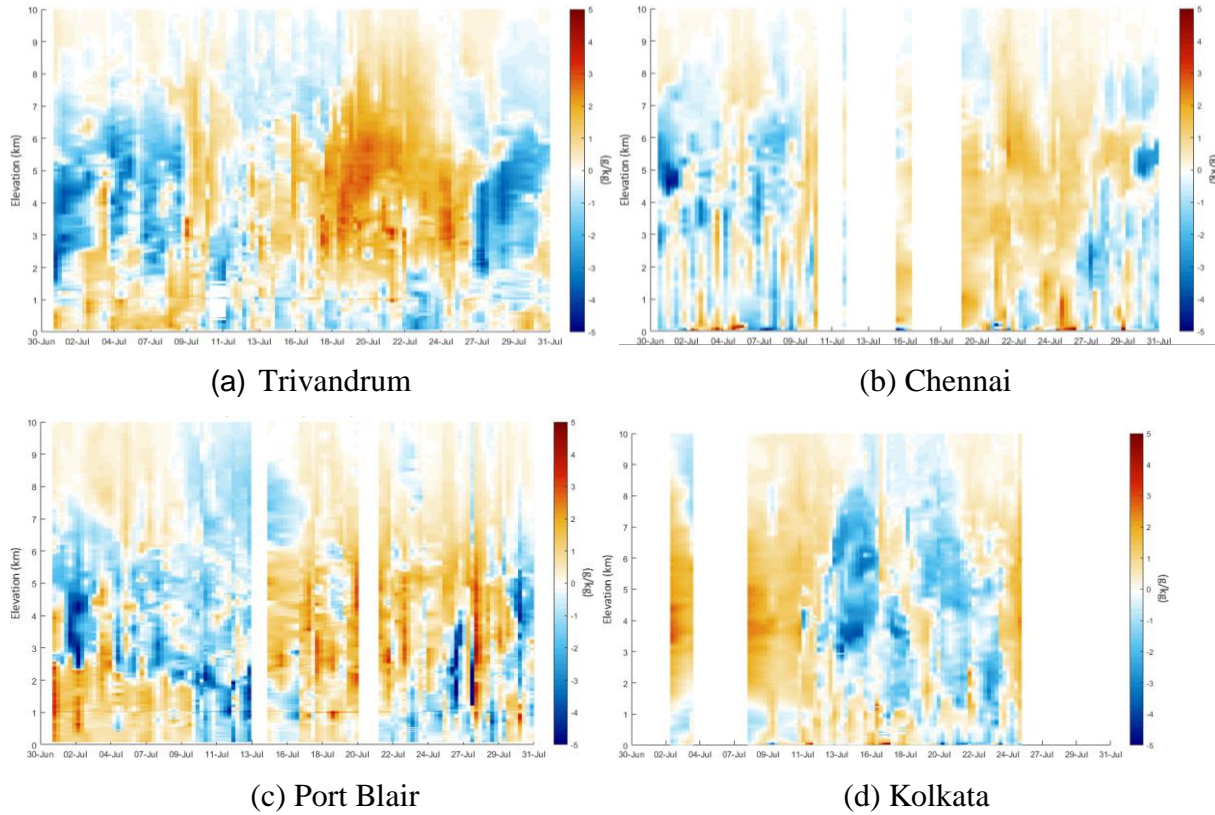


Figure 5: Specific humidity (kg/g) anomalies taken from radiosondes launched at Trivandrum, Chennai, Port Blair, and Kolkata, for July 2019. Colors indicate the relative wet (red) and dry (blue) phases of the atmosphere, respect to its mean monthly (July) value. Gaps between soundings with  $\leq 24$ hrs have been filled via temporal interpolation, with white gaps indicating the out of bounds gaps. Based on high frequency soundings from Indian Meteorological Departments (IMD), provided by Prof. G.N. Bhat, Indian Institute of Sciences.

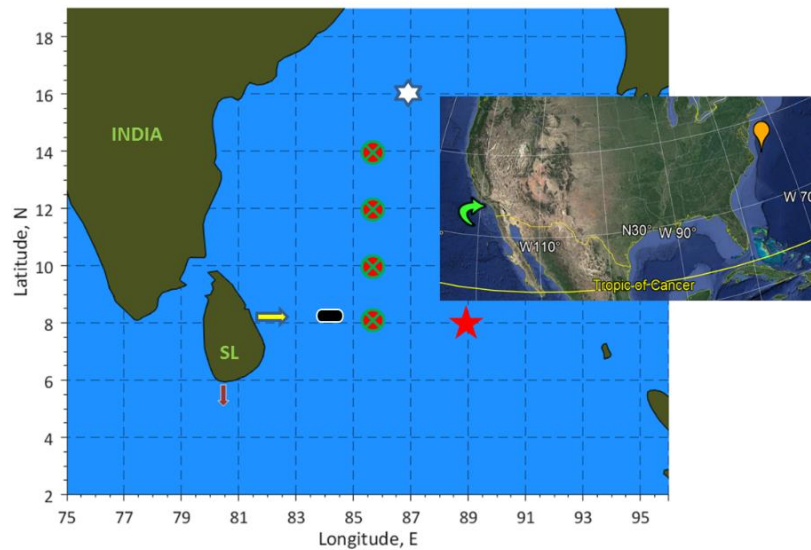


Figure 6: Locations of the VMP measurements taken in the BOB in 2013-2014 and 2018-2019: 1 - white star (2013, 16N/87E); 2 – brown arrow (2014, South of Weligama, in Southwest Monsoon Current,  $\sim 5.37\text{N}/80.4\text{E}$ ); 3 – light-yellow arrow (2014, off Trincomalee  $8.1\text{N}/82.6\text{E}$ ); 4 – dark-blue oval (2018, Sri Lanka Dome,  $8.1\text{N}/82.6\text{E}$ ); 5 – red-green crossed circles (2019, BOB,  $8\text{N}, 10\text{N}, 12\text{N}, 14\text{N}/85.75\text{E}$ ); 6 – red star (2019, southeastern BOB,  $8\text{N}/89\text{E}$ ). In the insert: in the Atlantic – orange bulb (2015, Gulf Stream Section GSs,  $85.8\text{N}/74.1\text{W}$ ) and Pacific – green curved arrow (2017, Southern California Bight SCB,  $33.76\text{N}/119\text{W}$ )

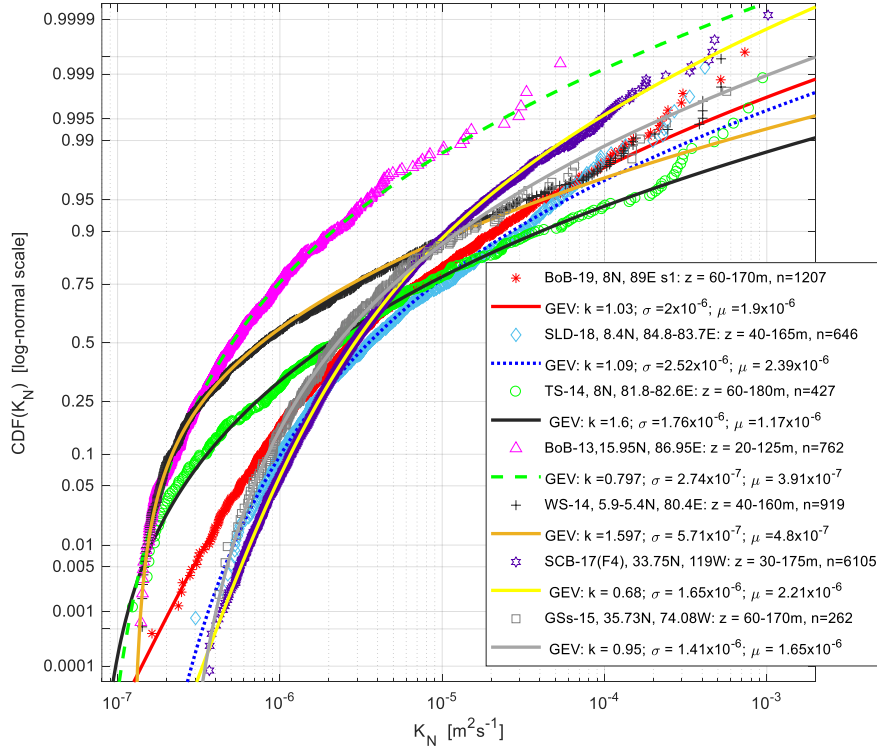


Figure 7: Cumulative distribution functions of the diffusivity  $CDF(K_N)$  in the upper pycnocline based on the dissipation and stratification measurements taken in several representative regions of the BoB in 2013-2014 and 2018-2019 using VMP-500 (see map in Fig. 1). The BoB probability distributions of the eddy diffusivity  $K_N$  are shown along with the pycnocline  $CDF(K_N)$  obtained in deep waters of the Southern California Bight (SCB-17) and the Gulf Stream Section (GSs-15). The depth ranges ( $z$ ) and a number of samples ( $n$ ) used for  $CDF(K_N)$  evaluation are in the legend. All observed probability functions are well approximated by generalized extreme value GEV distribution with the shape  $k$ , scale  $\sigma$ , and location  $\mu$  parameters given in the inset. Abbreviations: BoB-19 – Central BoB section, May 31-June 3, 2019; SLD-18 – Western BoB, including Sri Lanka Dome, July 16-17, 2018; TS-14 – East Indian Coastal Current Sep 9-10, 2014; BOB-13 – Northern BoB, Nov 18, 2013; WS-14 – South Monsoon Current, Weligama Section, April 23-24, 2014; SCB-17 (F4) – see above, Oct 4, 2017; GSs-15 – see above, Oct 30, 2015. Also refer to Figure 6 for location details. The eddy diffusivity was estimated as  $K_N = 0.2\varepsilon/N^2$  in the upper pycnocline, where the turbulent kinetic energy dissipation rate  $\varepsilon(z)$  and buoyancy frequency  $N(z)$  were obtained using VMP-500 casts.

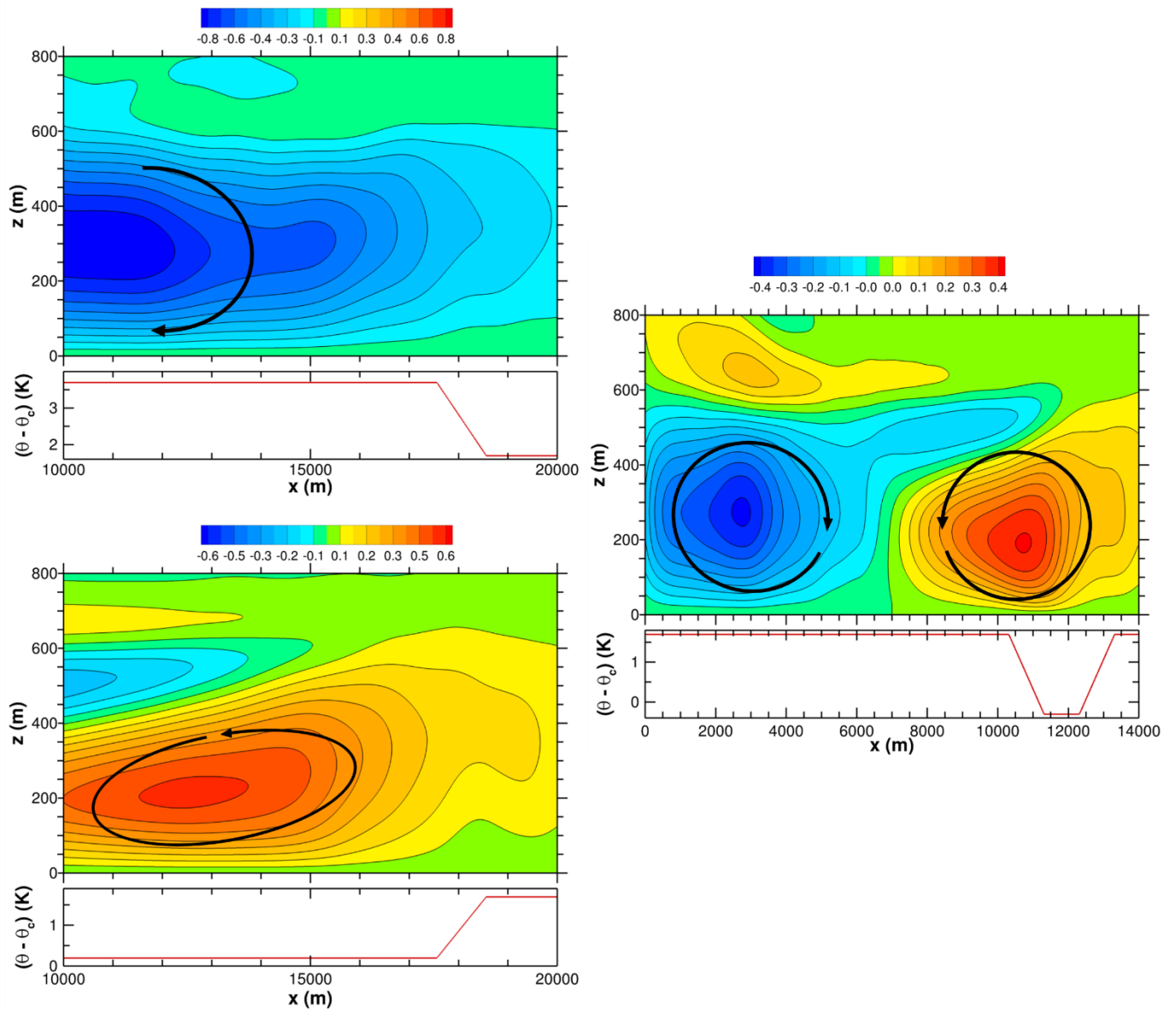


Figure 8: Stream function  $\psi_p$  computed from the secondary circulation wind from a simulation with down front winds above positive and negative SST jumps (upper and lower left panels, respectively), and a cold filament right panel. The shaded contours are evenly spaced. The black stream-trace highlights the average direction of the secondary circulation in each figure. The variation of the SST  $\langle \theta - \theta_c \rangle$  with  $x$  is shown in the lower panel of each figure. The far field ageostrophic wind  $\langle u \rangle$  is from right-to-left.

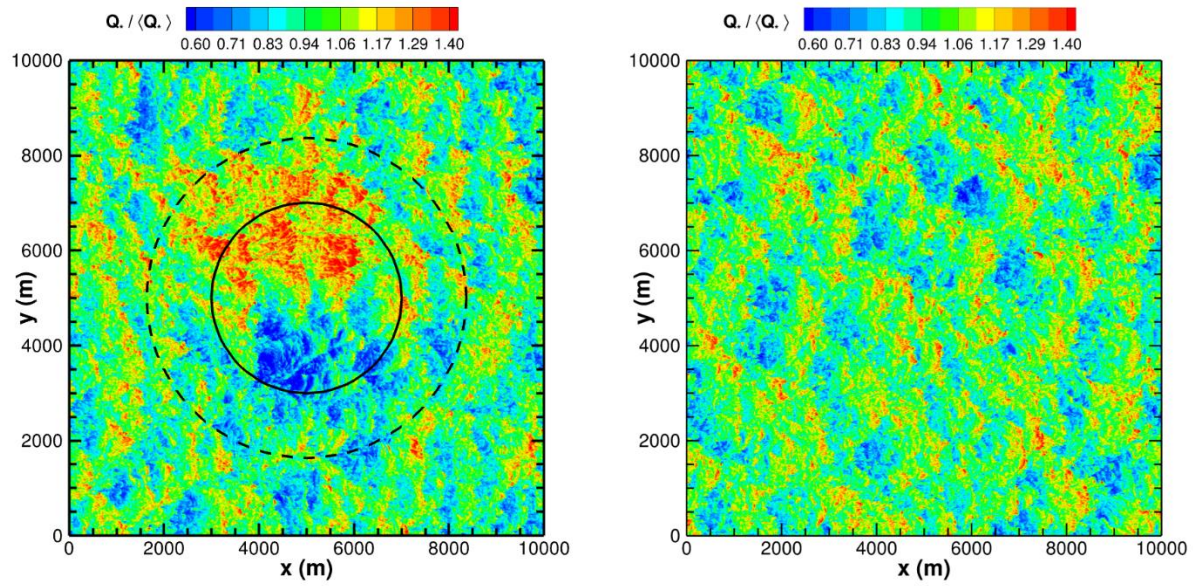


Figure 9: Snapshot of the instantaneous surface temperature flux  $Q^*$  above a circular water eddy (left panel) compared to  $Q^*$  with no currents (right panel). The maximum azimuthal current of 1 m/s is located at an eddy radius of approximately 2 Km indicated by the solid black circle. The dotted black circle indicates an azimuthal current of 0.2 m/s. The eddy rotation is cyclonic. The color bar is normalized by the average temperature flux  $\sim 0.013$  K m/s computed from a spatial average over the entire x-y plane for simulations with and without currents. The geostrophic winds are light 2.5 m/s from left-to-right. The enhanced fluctuations in the left panel are a consequence of coupling with the underlying water currents.